





Article

The Influence of Soil Physical Properties on the Load Factor for Agricultural Tractors in Different Paddy Fields

Yi-Seo Min ¹, Yeon-Soo Kim ², Ryu-Gap Lim ³, Taek-Jin Kim ⁴, Yong-Joo Kim ^{5,6,*} and Wan-Soo Kim ^{1,7,*}

¹ Department of Bio-Industrial Machinery Engineering, Kyungpook National University, Daegu 41566, Republic of Korea; msg337@gmail.com

² Department of Bio-Industrial Machinery Engineering, Pusan National University, Miryang 50463, Republic of Korea; yskim23@pusan.ac.kr

³ Department of Smart Agriculture, Korea Agriculture Technology Promotion Agency, Iksan 54667, Republic of Korea; limso@koat.or.kr

⁴ Department of Drive System Team, TYM R&D Center, Iksan 54576, Republic of Korea; taek.kim@tym.world

⁵ Department of Smart Agriculture Systems, Chungnam National University, Daejeon 34134, Republic of Korea

⁶ Department of Biosystems Machinery Engineering, Chungnam National University, Daejeon 34134, Republic of Korea

⁷ Upland Field Machinery Research Center, Kyungpook National University, Daegu 41566, Republic of Korea

* Correspondence: babina@cnu.ac.kr (Y.-J.K.); wansoo.kim@knu.ac.kr (W.-S.K.)

Abstract: The load factor (LF) of a tractor represents the ratio of actual engine power and rated engine power, and is an important indicator directly used in calculating national air pollutant emissions. Currently, in the Republic of Korea, a fixed value of 0.48 is used for the LF regardless of the working conditions, making it difficult to establish a reliable national air pollutant inventory. Since tractors perform work under soil conditions, soil physical properties directly affect the tractor LF. Therefore, it is expected that more accurate LF estimation will be possible by utilizing soil physical properties. This study was conducted to assess the impact of soil physical properties on the LF. Experimental data were collected in ten different soil conditions. Correlation analysis revealed that the LF exhibited strong correlations with SMC, soil texture, and CI, in that order. The coefficient of determination for the regression model developed using soil variables ranged from 0.678 to 0.926. The developed regression models generally showed higher accuracy when utilizing multiple soil variables, as compared to using a single soil variable. Therefore, an effective estimation of the LF through non-experimental methods can be achieved by measuring various soil properties.

Keywords: agricultural tractor; load factor; engine characteristic; soil physical properties; tillage operation



Citation: Min, Y.-S.; Kim, Y.-S.; Lim, R.-G.; Kim, T.-J.; Kim, Y.-J.; Kim, W.-S. The Influence of Soil Physical Properties on the Load Factor for Agricultural Tractors in Different Paddy Fields. *Agriculture* **2023**, *13*, 2073. <https://doi.org/10.3390/agriculture13112073>

Academic Editor: Jin He

Received: 27 September 2023

Revised: 24 October 2023

Accepted: 26 October 2023

Published: 29 October 2023



Copyright: © 2023 by the authors. Licensee MDPI, Basel, Switzerland. This article is an open access article distributed under the terms and conditions of the Creative Commons Attribution (CC BY) license (<https://creativecommons.org/licenses/by/4.0/>).

1. Introduction

Recently, there has been a significant amount of international interest in addressing environmental pollution problems [1]. The Korean government provides a clean air policy support system (CAPSS) for the management of national air pollutant emissions to analyze emissions and uses it to utilize national air conservation policies [2]. NRMS by non-road mobile machinery (NRMM), including agricultural machinery and construction machinery, is one of the key categories among the various sectors managed by CAPSS [3]. The Republic of Korea's NO_x emissions from NRMMs were 311,748 tons in 2019, which is 28.7% of the country's annual NO_x emissions [4].

Among the various machinery industries included in NRMM, agricultural machinery is essential for the production of high-efficiency and high-quality agricultural products. Tractors are among the most useful agricultural machinery. In 2019, the annual working area of tractors in the Republic of Korea was 21.7 ha/year, and the annual usage time was 139.9 h/year [5]. They can be specifically employed to perform multi-purpose agricultural tasks by attaching various pieces of working equipment [6].

In the Republic of Korea, national air pollutant emissions from agricultural machinery are calculated using the following formula [3,7], which takes into account the number of units owned, rated power, load factor (LF), and emission factor: $\text{Emission (g/y)} = \text{Number of machinery} \times \text{Rated power (kW)} \times \text{Load factor} \times \text{Working hours (h/y)} \times \text{Emission factor (g/kWh)}$. LF is one of the most important factors in the above formula [8]. It is a quantitative indicator of the average power rating of the engine [9,10]. Currently, in the Republic of Korea, LF is used as a fixed value of 0.48 regardless of various conditions, such as the agricultural machinery type, model, power range, and operating conditions [11]. This greatly reduces the reliability of the national emissions inventory for agricultural machinery, and it is necessary to secure an LF generated under actual agricultural working conditions for an accurate representation.

In the domain of construction machinery, there have been studies aimed at quantifying the LF and emissions under actual operational conditions. Previous studies have indicated that the LF and emissions during actual operations are contingent on the specific type of construction equipment [12]. The conclusions of this study propose the potential for devising an emission factor model based on the LF. However, due to the influence of diverse emission control devices, the linear relationship between LFs and emission factors has proven elusive [13]. Barati and Shen (2016) developed an LF estimation model and an emission estimation model [14]. The LF model was developed using three operating parameters, including machine acceleration, road inclination, and machine speed, and the model demonstrated a high R^2 range of 0.973 to 0.986. And the emission model for CO_2 , Co, HC, and NO_x emission based on the LF exhibited a substantial R^2 range of 0.904 to 0.954. The conclusion of this study was that the LF and emissions have a strong linear relationship, and operational parameters have a high linear relationship with the LF, which suggests that emissions can be accurately estimated through operating parameters. As these operational parameters are crucial to the accuracy of the model, they should be selected taking into consideration the machine's characteristics.

Tractors are mainly operated in soil conditions, and the tractor's load (i.e., the LF) varies greatly depending on the soil conditions [15,16]. Numerous previous studies have indicated that the engine load differs depending on the soil physical properties. Inchebron et al. (2012) evaluated the traction performance of a tractor equipped with a moldboard plow at various tillage depths and SMC conditions [17]. It was demonstrated that elevated soil moisture content (SMC) led to increased rolling resistance and wheel slippage and decreased traction efficiency. Kim et al. (2021) analyzed the effect of SMC on tractor traction performance during moldboard plow operations [18]. The results of the study highlighted that the tractor's traction load varied in accordance with SMC levels. Rasool and Raheman (2018) conducted a study on improving the traction performance of mobile tractors according to the cone index (CI) [19]. The traction performance was assessed by towing a load tractor on the experimental tractor. It was identified that soils with a large CI increased the drawbar force and traction efficiency. Battiato and Diserens (2017) performed the simulation and validation of tractor traction performance under different soil texture conditions [20]. Traction tests were performed using a second tractor as a braking machine. As a result, the traction power of the tractor was found to be different in soils with different soil textures.

In previous studies, the emphasis was primarily on tractor wheel slip and traction force. Multiple soil variables were employed to describe the LF of the tractor. The soil physical properties have intricate interactions with the soil–tractor system, making it challenging to mathematically resolve these relationships. Consequently, numerous studies in terramechanics have been conducted based on empirical experimental values, primarily focusing on individual soil variables. While individual soil physical characteristics can influence the LF, employing a broader range of soil variables could provide a more comprehensive explanation of the engine load of the tractor [21,22]. Previous research indicates that SMC, CI, and soil texture are interrelated, and this relationship appears to be nonlinear [23]. In specific soil conditions, an increase in SMC can initially lead to an increase in CI, followed

by a decrease, which is influenced by the soil's particle composition. These characteristics make it challenging to predict the impact of unaccounted soil conditions on the LF. Therefore, estimating tractor load based on various combinations of soil conditions can enhance a model's reliability. However, this approach has limitations due to the difficulty of obtaining soil and engine load data. Consequently, comprehensive studies that evaluate tractor LF based on diverse combinations of soil conditions are relatively scarce.

Research on the influence of soil physical properties on tractor LFs can aid in the appropriate estimation of the LF based on soil variables. Due to the highly diverse and challenging-to-control nature of soil conditions, it is impractical to experimentally evaluate the LF across all soil conditions. Estimating the LF using tractor specifications and soil variables could lead to more accurate exhaust gas emission calculations compared to applying a fixed value of 0.48. This may help to improve the reliability of emission data from tractors in the Republic of Korea.

Therefore, the aim of this study is to evaluate the effect of soil physical properties on the LF of tractors. This study is expected to provide useful information as a foundational study for estimating the tractor LF based on soil physical properties in the future. The specific objectives of this study are as follows: (1) the measurement of tractor engine data using a load measurement system, (2) the measurement of soil physical properties, (3) an evaluation of the influence of soil physical properties on the tractor LF, and (4) the development of an LF estimation model according to soil properties.

2. Materials and Methods

2.1. Experimental Equipment

2.1.1. Agricultural Tractor

In this study, a 78 kW agricultural tractor (S07, TYM, Gongju, Republic of Korea) was utilized. Table 1 details the specific tractor specifications utilized in this study. Figure 1 depicts the engine performance curve of the tractor.

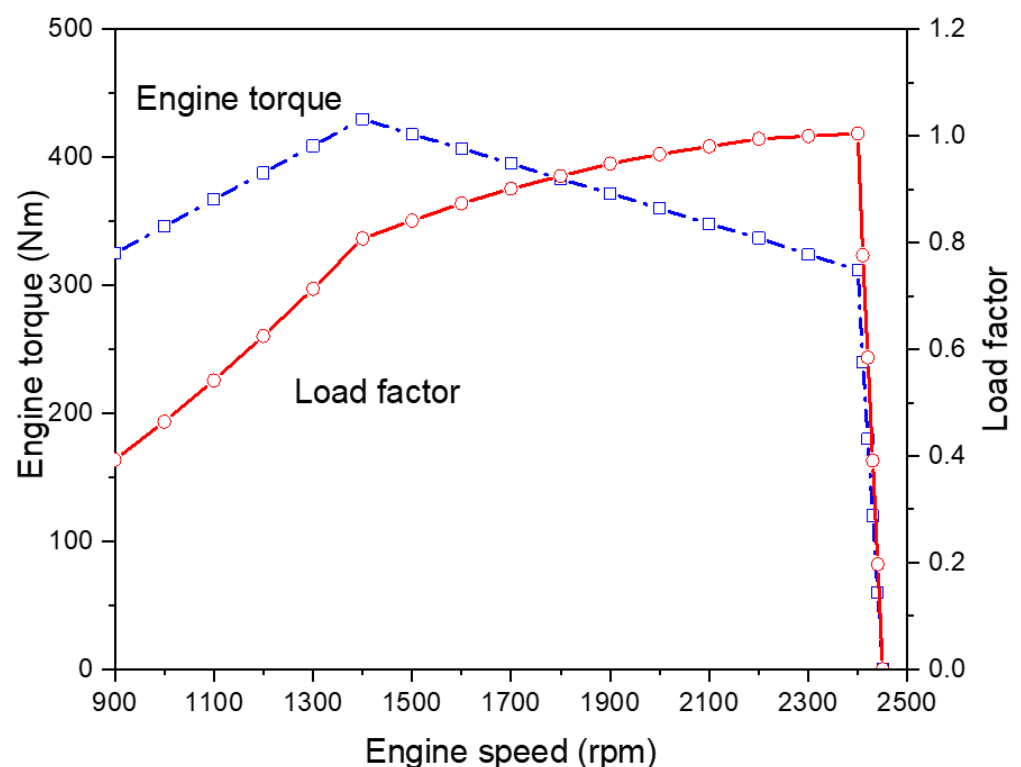


Figure 1. The engine performance curve of the tractor used in this study.

Table 1. Specification of the 78 kW agricultural tractor used in this study.

Item		Specifications
Engine	Dimensions (length × width × height) (mm)	4225 × 2140 × 2830
	Empty weight (kg)	3985
	Make	DOOSAN INFRACORE
	Type	In-line, 4-cycle
	Aspiration	Turbocharged and intercooler
	Rated torque (Nm)	324 @2300 rpm
	Rated power (kW)	78 @2300 rpm
	Max. torque (Nm)	430 @1400 rpm
	Torque rise (%)	31.3
	Maximum speed (rpm)	2450
	Bore × Stroke (mm)	98 × 113
	Total displacement (cc)	3409
	Compression ratio	17:1
	Dry weight (kg)	500
	Emission Compliance	TIER4-Final/EU STAGE IV
Transmission	Type	Power shuttle
	Gear stage (Forward/Reverse)	32/32

2.1.2. Measurement Equipment

In this study, a tractor equipped with a Tier-4 compliant electronic control unit was utilized. Engine torque and engine rotational speed during field operations were measured using a data measurement device (QuantumX MX840B, HBM, Darmstadt, Germany) through controller network area (CAN) communication. Among various soil physical properties, we selected three representative attributes: SMC, CI, and soil texture. SMC was measured through a soil moisture sensor (TDR350; Spectrum Technology, Aurora, IL, USA) with two rods, each 20 cm in length. CI was measured with a cone penetrometer (SC900; Spectrum Technology, Aurora, IL, USA). The average CI value, calculated from measurements obtained every 25 mm at a depth of 150 mm, was employed [24]. Table 2 demonstrates the specifications of the soil measurement equipment. Soil samples were collected at a depth of 150 mm. The soil particle proportion was determined using the hydrometer method of the Soil Environment Analysis Center of Chungnam National University, and soil texture was classified according to the USDA soil classification system.

Table 2. Specification of the soil measurement equipment used in this study.

Item	Specification
Soil moisture sensor	Measurement units: percentage of volumetric water content (VWC)
	Range: 0% VWC to saturation
	Accuracy: ±3.0% VWC
Cone penetrometer	Measurement units: cone index (kPa)
	Range: 0 to 45 cm, 0 to 7000 kPa
	Accuracy: ±1.25 cm, ±103 kPa

2.2. Field Experiment

2.2.1. Field Site

The field experiment was conducted at 10 sites in the Republic of Korea, as illustrated in Figure 2. All sites were paddy fields where rice was the primary crop, and only stubble remained at the time of the experiment. The experiments were conducted in March of the experimental year, just before the rice was transplanted, following the November harvest of the previous year. Information for each site is presented in Table 3.

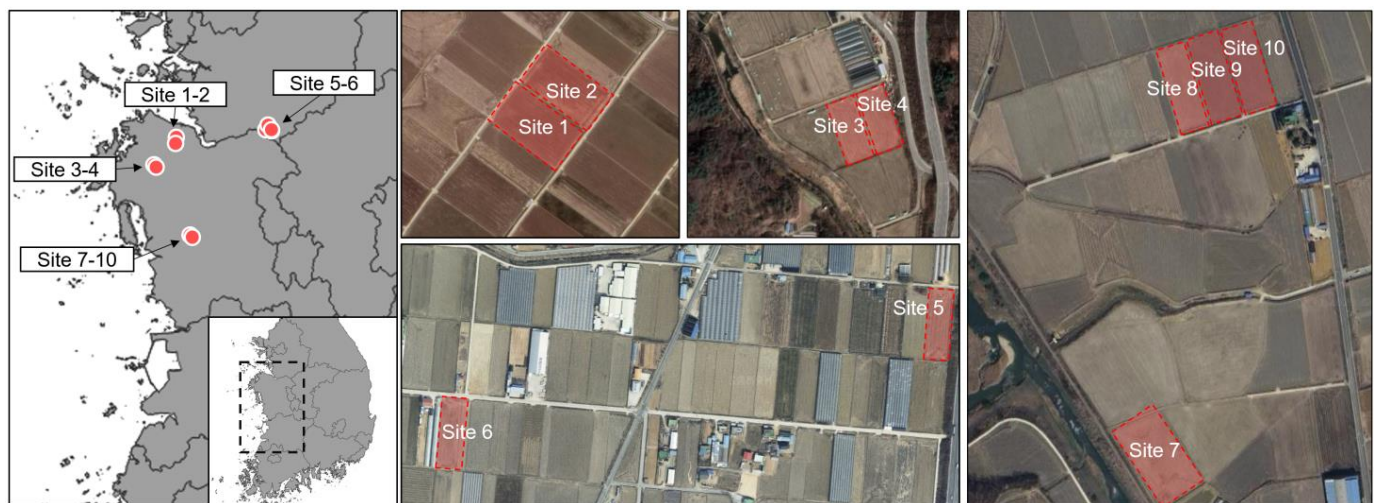


Figure 2. Geospatial information of each experimental site.

Table 3. Information about the field experiment sites.

Sites	Field Size (m)	Location	Latitude	Longitude	Experimental Year
1	60 × 100	Seosan	36°46′44.4″ N	126°33′27.0″ E	2017
2	60 × 100	Seosan	36°46′46.2″ N	126°33′28.8″ E	2017
3	40 × 100	Cheongyang	36°30′35.3″ N	126°47′27.5″ E	2017
4	40 × 100	Cheongyang	36°30′35.9″ N	126°47′29.1″ E	2017
5	30 × 100	Anseong	36°56′42.7″ N	127°14′33.2″ E	2019
6	40 × 100	Anseong	36°56′37.8″ N	127°14′04.5″ E	2019
7	60 × 100	Dangjin	36°55′50.0″ N	126°37′57.5″ E	2019
8	40 × 100	Dangjin	36°56′04.1″ N	126°37′58.3″ E	2019
9	40 × 100	Dangjin	36°56′04.3″ N	126°37′59.8″ E	2019
10	40 × 100	Dangjin	36°56′04.8″ N	126°38′01.5″ E	2019

2.2.2. Soil Environment Measurement

Soil sampling can be carried out using various methods, including simple random sampling, systematic sampling, and stratified sampling. Samples are collected according to a regularized pattern in systematic sampling [25]. This method is often more accurate than simple random sampling because it guarantees uniform spatial coverage [26]. Therefore, in this study, soil samples were collected using a systematic sampling method. A total of ten soil samples were collected from each of the ten field sites, and SMC and CI were measured at the same points.

2.2.3. Field Experiment Conditions

In this study, the tractor implement used was an eight-blade moldboard plow (WJSP-8; Woongjin Machinery, Gimje, Republic of Korea). The dimensions of the moldboard plow were 2150 mm × 2800 mm × 1250 mm (length × width × height), with a weight of 790 kg. The tractor's driving gear stage was set to M3 low (7.09 km/h) during plow tillage [8]. The tillage depth was set to be in the range of 13 to 17 cm through the tractor's automatic tilling depth control system, and tillage work was performed with an average tillage depth of 15 cm.

2.3. Data Analysis

2.3.1. Load Factor Analysis

Engine torque and rotational speed data collected during tractor operations in the ten sites were analyzed to determine the LF. The engine power was calculated as in Equation (1), using time-based engine torque and rotational speed. Then, the average of engine power

was calculated using time-based engine power. The analysis process of the engine power involved removing outliers using boxplot-based whisker analysis. In particular, this process was used to remove engine power values that were higher than the engine's rated power. The average of engine power data for each site was used in calculating the LF, as shown in Equation (2). One-way analysis of variance (ANOVA) was performed using IBM SPSS Statistics (SPSS 25, SPSS Inc., New York, NY, USA) to evaluate whether soil physical property and engine characteristic data from each site showed significant mean differences between groups.

$$EP = \frac{2\pi TN}{60,000}, \quad (1)$$

$$LF = \frac{EP_m}{EP_r}, \quad (2)$$

where EP represents the engine power, T is the engine torque, N is the engine rotational speed, LF is the load factor, EP_m is the measured engine power in real time, and EP_r is the rated engine power.

2.3.2. Correlation Analysis

A correlation analysis was conducted to analyze the impact of soil physical properties on the LF. The linearity between two variables was assessed using the Pearson correlation coefficient (r), as illustrated in Equation (3). The range of r values is from -1 to 1 , where an absolute value of 1 indicates a perfect linear relationship and a value of 0 signifies no linear relationship. Each soil variable is considered to have a linear relationship with the LF when the absolute value of r is 0.7 or higher and the significance level of $p < 0.05$.

$$r = \frac{\sum_{i=1}^n (X_i - \bar{X})(Y_i - \bar{Y})}{\sqrt{\sum_{i=1}^n (X_i - \bar{X})^2 \sum_{i=1}^n (Y_i - \bar{Y})^2}} \quad (3)$$

where \bar{X} is the mean of sample group X , and \bar{Y} is the mean of sample group Y .

2.3.3. Regression Analysis

The data collected from field experiments were used to develop regression models. Since the tractor and equipment conditions were consistent throughout the experiments, only soil variables were considered in the regression models. Considering the ease of data collection for each soil variable, regression models were constructed using both individual functions and combinations of functions. Equation (4) can be utilized in cases when only a soil moisture sensor is accessible. Equation (5) can be utilized in cases when only a soil strength sensor is accessible. Soil moisture sensors and soil strength sensors have been widely used as important tools for soil monitoring due to their affordability and ease of measurement. Equation (6) can be utilized when analyzing soil texture of an experimental field. The soil texture incorporates the proportions of sand, silt, and clay, but we only considered the sand proportion, which has the most significant impact on the LF. Using multiple soil texture variables had a detrimental effect on the model's performance, as stated in the paper. Typically, soil texture analysis involves several processes, such as sample collection, drying, and classification, making data measurement more challenging. Furthermore, in order to investigate whether the estimation performance of the model was enhanced by combining multiple soil variables, we employed all possible combinations of these variables ($f_1, f_2, f_3, f_1 + f_2, f_1 + f_3, f_2 + f_3, f_1 + f_2 + f_3$), as stated in the study.

$$LF = f_1(\text{SMC}) \quad (4)$$

where SMC is the soil moisture content.

$$LF = f_2(\text{CI}), \quad (5)$$

where CI is the cone index.

$$LF = f_3(S_a) \quad (6)$$

where S_a is the sand proportion.

The performance of the estimative model based on regression analysis was evaluated by referring to previous studies. For the assessment of model performance, four statistical metrics were chosen: the coefficient of determination (R^2), mean absolute percentage error (MAPE), root mean square error (RMSE), and relative deviation (RD) [27]. Each of these model performance metrics was calculated using Equations (7)–(10), based on the actual and estimated engine loads.

$$R^2 = \frac{\sum_{i=1}^N (y_i - y_a) - \sum_{i=1}^N (y_i - \hat{y}_i)}{\sum_{i=1}^N (y_i - y_a)}, \quad (7)$$

$$MAPE = \frac{1}{N} \sum_{i=1}^N \left| \frac{1}{y_i} (y_i - \hat{y}_i) \right| \times 100(\%), \quad (8)$$

$$RMSE = \sqrt{\frac{1}{N} \sum_{i=1}^N (\hat{y}_i - y_i)^2}, \quad (9)$$

$$RD = \frac{RMSE}{\text{Mean}} \times 100, \quad (10)$$

where y_a is the mean actual load factor, y_i is the actual load factor, and \hat{y}_i is the estimated load factor.

3. Results

3.1. Soil Physical Properties

The collected CI and SMC from a total of ten sites are displayed in Figure 3. The CI and SMC exhibited large variations across ten measurements for each site. In terms of the CI, the largest variation was observed at site 9, ranging from 640.6 to 2085.0 kPa. As for the SMC, the most extensive range was observed at site 1, ranging from 24.2 to 41.0%. Additionally, in general, the CI exhibited a wider range than the SMC. The minimum value for CI was observed at site 4, measuring 236.6 kPa, while the maximum value was observed at site 9, measuring 2085.0 kPa. For SMC, the minimum value was noted at site 4, measuring 18.42%, while the maximum value was noted at site 8, measuring 45.90%.

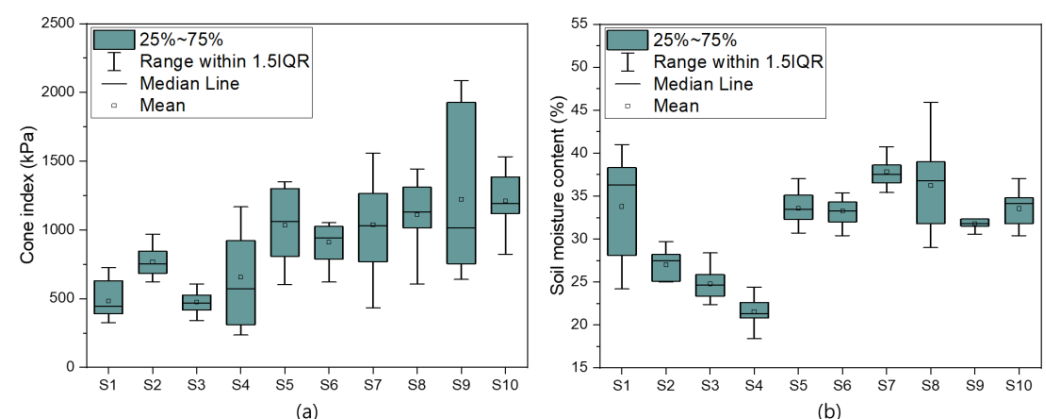


Figure 3. Results of box plot analysis of soil physical properties measured on field experiment sites (e.g., S1 refers to site 1): (a) cone index (CI) and (b) soil moisture content (SMC).

Figure 4 illustrates the results of the particle distribution proportion analysis for each particle type in the context of soil texture analysis. The sand proportion ranged from 24% to 85% across all sites, with Groups S1 to S4 exhibiting a sand proportion of over 70%. The

silt proportion ranged from 13% to 57% across all sites, while Groups S5 to S10 displayed higher silt proportions, exceeding 35%. Clay ranged from 2% to 27%, with Groups S1 to S4 demonstrating a low clay proportion of less than 8%, and Groups S5 to S10 demonstrating a high clay proportion of over 18%. Sites with a high sand proportion exhibited relatively low CI values. These results are consistent with findings reported in previous studies [28].

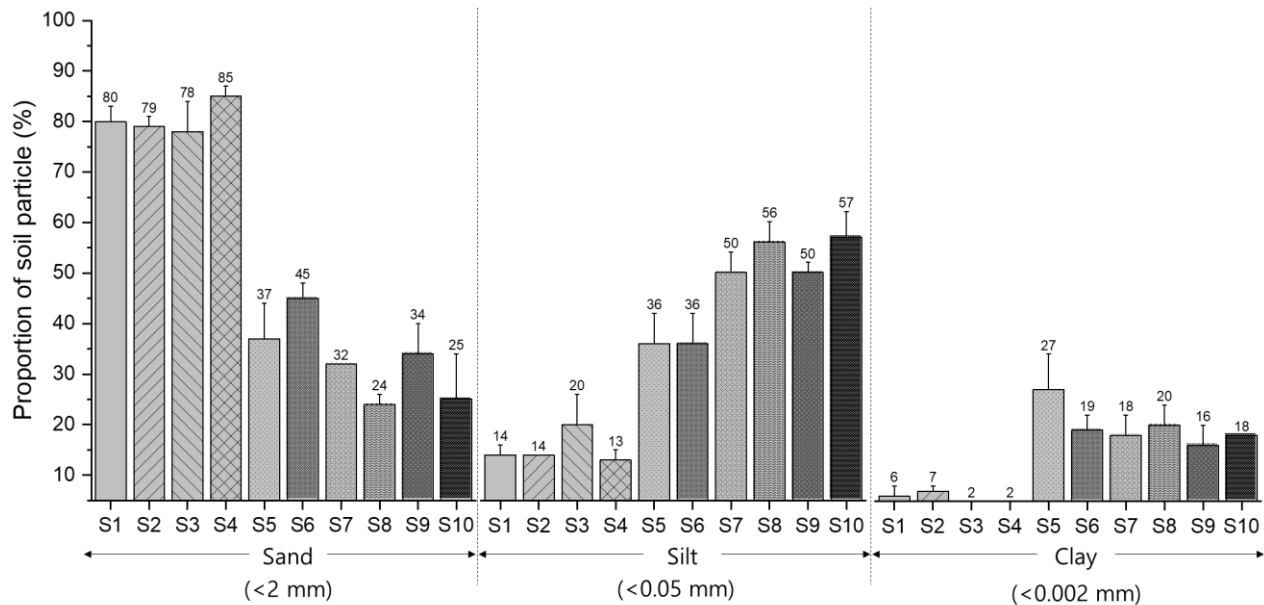


Figure 4. Results of sand, silt, and clay proportion analysis of soil particles by field experiment sites, where S# refers to the number of sites (i.e., S1 = Site 1).

Table 4 presents the analysis results of the soil physical properties of the ten sites used in this study. Soil textures were categorized as loamy sand in four sites, clay loam in one site, loam in two sites, and silt loam in three sites. An ANOVA analysis was conducted to determine whether there were significant differences in the means of soil physical properties data across different sites. The analysis results indicated statistically significant differences between sites, with the exception of a few sites with comparable values. Furthermore, in all cases except for the comparison between sites 8 and 10, each site exhibited statistically significant mean differences in at least one soil physical property. This suggests that data measurements were taken from sites with varying soil physical properties.

Table 4. Analysis results of averaged soil physical properties, including soil moisture content, cone index, soil particle proportions, and soil texture (N = 10).

Sites	SMC (%)	CI (kPa)	Soil Particle Proportions (%)			Soil Texture
			Sand (<2 mm)	Silt (<0.05 mm)	Clay (<0.002 mm)	
1	33.79 ^{b,c}	483 ^e	80.00 ^b	14.00 ^e	6.00 ^d	Loamy sand
2	27.01 ^d	768 ^{c,d}	79.00 ^b	14.00 ^e	7.00 ^d	Loamy sand
3	24.79 ^d	476 ^e	78.00 ^b	20.00 ^d	2.00 ^e	Loamy sand
4	21.55 ^e	656 ^{d,e}	85.00 ^a	13.00 ^e	2.00 ^e	Loamy sand
5	33.60 ^{b,c}	1034 ^{a,b,c}	37.00 ^d	36.00 ^c	27.00 ^a	Clay loam
6	33.27 ^c	910 ^{b,c,d}	45.00 ^c	36.00 ^c	19.00 ^b	Loam
7	37.84 ^a	1038 ^{a,b,c}	32.00 ^e	50.00 ^b	18.00 ^{b,c}	Loam
8	36.24 ^{a,b}	1111 ^{a,b}	24.00 ^f	56.00 ^a	20.00 ^b	Silt loam
9	31.77 ^c	1223 ^a	34.00 ^e	50.00 ^b	16.00 ^c	Silt loam
10	33.54 ^{b,c}	1212 ^a	25.00 ^f	57.00 ^a	18.00 ^{b,c}	Silt loam

Mean values within same column showing different superscripts are significantly different ($p < 0.05$). Duncan's least significant multiple-range test was employed to compare the means.

Figure 5 displays the results of mapping the 10 study sites onto the USDA soil texture classification triangle. Overall, sites 1–4 are predominantly situated within the loamy sand region, characterized by high sand proportions and low clay proportions. The remaining sites exhibited a balanced mixture of soil particles.

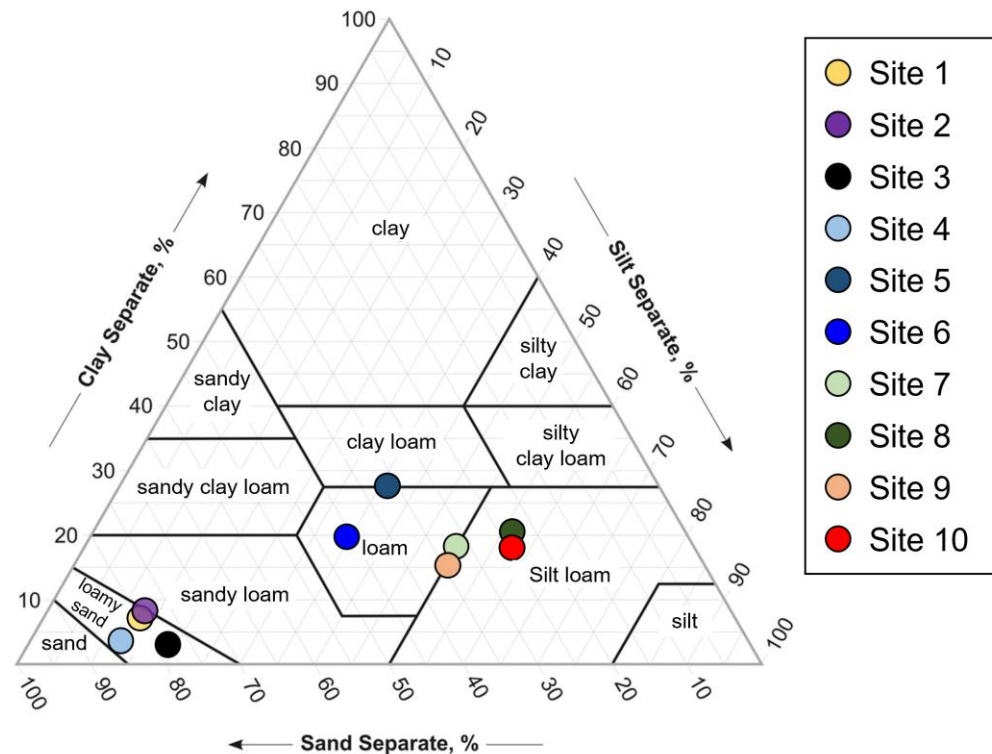


Figure 5. Classification results of the sampled soil by ten field experiment study sites mapped to the USDA soil texture triangle.

3.2. Engine Load Characteristics

The measurement results of the engine load characteristics at each site are depicted in Figure 6. Site 4 had the lowest average engine torque of 127.1 Nm, while site 7 had the highest average engine torque of 359.1 Nm. Site 6 had the lowest average engine rotational speed at 1967 rpm, while site 4 had the highest at 2450 rpm. The average engine power and average LF were lowest at site 4, measuring 32.60 kW and 0.418, respectively, and highest at site 10, measuring 78.33 kW and 1.004, respectively. The engine power and LF exhibited a similar box plot pattern to that of engine torque. Therefore, engine torque is estimated to have a greater effect on LF than engine rotation speed.

The statistical analysis results of the engine load characteristics are presented in Table 5. The average values of the engine load characteristics across all sites ranged as follows: engine rotation speed from 2148 to 2419 rpm, engine torque from 227.2 to 329.7 Nm, engine power from 57.52 to 76.76 kW, and LF from 0.737 to 0.984. According to the ANOVA results, both engine rotation speed and engine torque exhibited statistically significant mean differences across all sites. Conversely, there were no statistically significant differences observed in engine power and LF between sites 7 and 8 or between sites 5 and 9.

Figure 7 displays the results of mapping the average LF for each site to the engine performance curve. During soil tillage operations, tractors are generally operated at an engine rotational speed of 2400 rpm; however, when there is a demand for a higher load than the LF that can be output at this time, the engine rotational speed is reduced to output a higher LF [29]. Therefore, site 4, which has a low LF requirement, performs work in the range of 2400 rpm, whereas sites with a higher LF requirement have an engine operating point in a lower range of engine rotation speed.

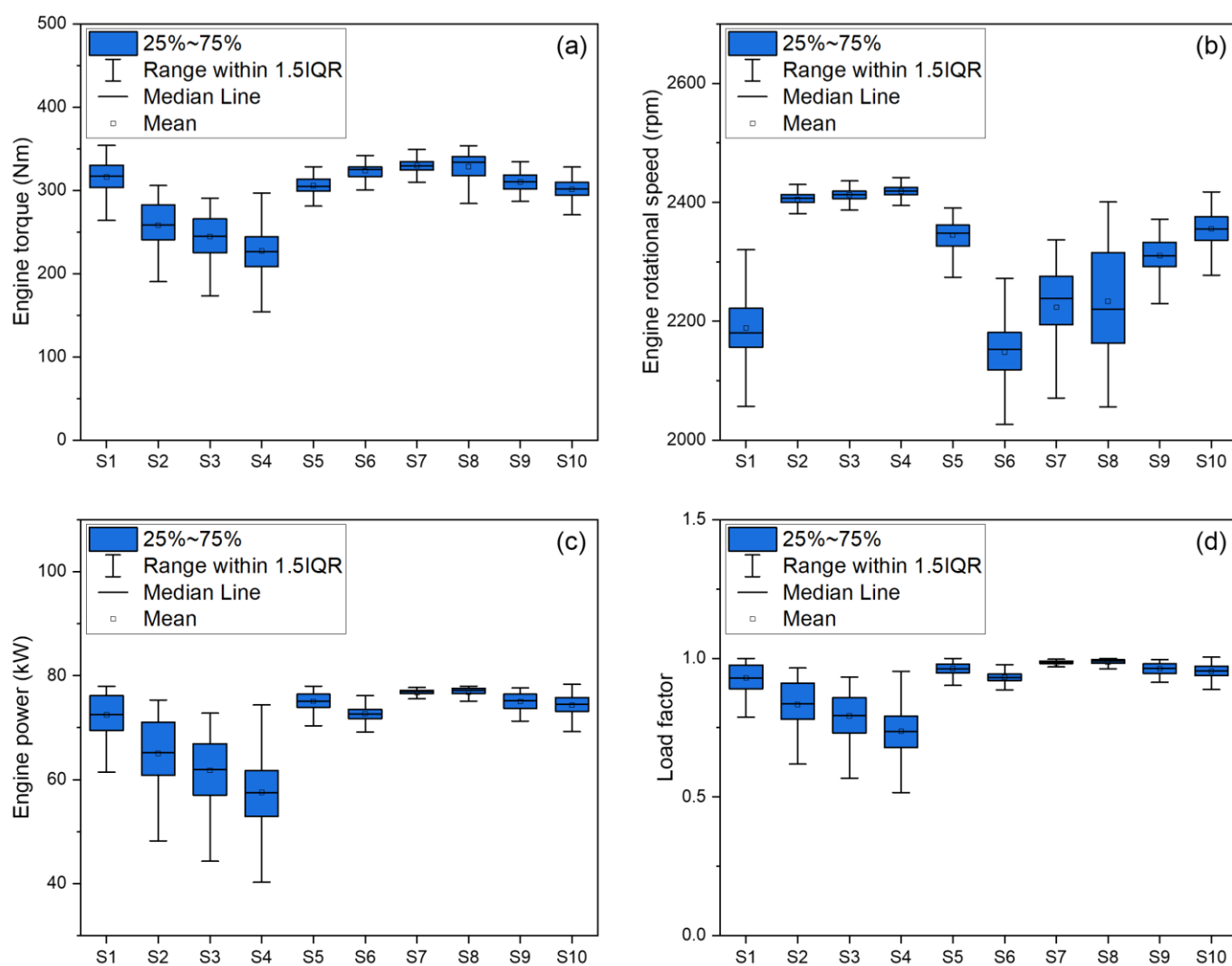


Figure 6. Results of box plot analysis of engine load measured on field experiment sites (e.g., S1 refers to site 1): (a) engine torque (ET), (b) engine rotation speed, (c) engine power (EP), and (d) load factor (LF).

Table 5. Results of engine load characteristics.

Sites	Engine Rotational Speed (rpm)	Engine Torque (Nm)	Engine Power (kW)	Load Factor
1	2189 ⁱ	316.4 ^d	72.47 ^e	0.929 ^e
2	2405 ^c	258.3 ^h	65.03 ^f	0.834 ^f
3	2413 ^b	244.6 ⁱ	61.77 ^g	0.792 ^g
4	2419 ^a	227.2 ^j	57.52 ^h	0.737 ^h
5	2345 ^e	305.8 ^f	75.07 ^b	0.962 ^b
6	2148 ^j	323.4 ^c	72.70 ^d	0.932 ^d
7	2224 ^h	329.7 ^a	76.71 ^a	0.983 ^a
8	2233 ^g	328.8 ^b	76.76 ^a	0.984 ^a
9	2310 ^f	310.3 ^e	75.05 ^b	0.962 ^b
10	2356 ^d	301.4 ^g	74.32 ^c	0.953 ^c

Means (\pm standard deviation) within same column showing different superscripts are significantly different ($p < 0.05$). Duncan's least significant multiple-range test was applied to compare the means.

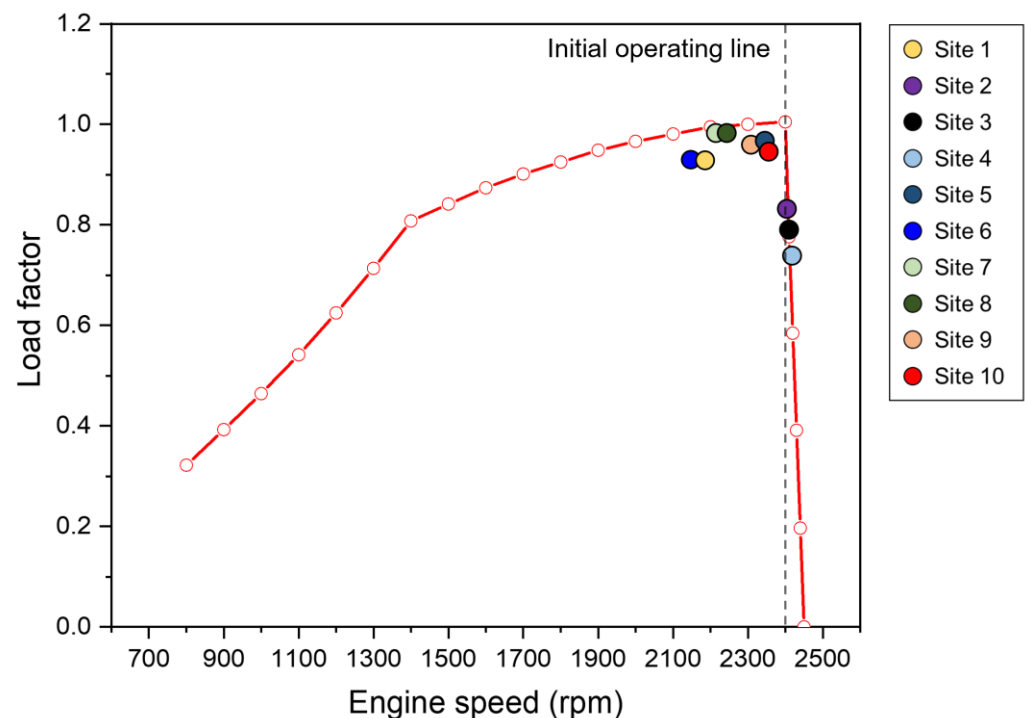


Figure 7. Load factor analysis results for each site on the engine performance curve.

3.3. Effect of Soil Physical Properties on Engine Load

Figure 8 presents the correlation matrix depicting the relationship between soil physical properties and engine load characteristics. The top portion of the matrix features bivariate scatterplots along with fitted lines, while the bottom section displays Pearson correlation coefficients. The engine speed exhibited a significance level of $p > 0.05$ between soil texture (sand, silt, and clay proportions) and the CI. Therefore, the correlation coefficients between engine speed and soil parameters are considered unreliable. In contrast, engine torque, engine power, and LF exhibited a significance level of $p < 0.05$ for all soil variables in the study. The LF exhibited correlation coefficients ranging from absolute values of 0.79 to 0.91 for soil parameters. Excluding engine power, the variables that had the most significant impact on the LF were engine torque ($r = 0.96$), SMC ($r = 0.91$), sand proportion ($r = -0.85$), and clay proportion ($r = 0.84$). Except for silt proportion and SMC, five of the soil variables mostly demonstrated a significance level of $p < 0.05$. The sand proportion and silt proportion displayed a very strong correlation coefficient of -0.98 . Therefore, to address the issue of multicollinearity in the regression model, only sand proportion, one of the two soil variables with a higher correlation coefficient with load, was selected as the soil variable for developing the regression model.

Table 6 presents the developed regression models. The adjusted R^2 ranges from 0.638 to 0.902, indicating that each model can estimate the load rate with an accuracy ranging from 63.8% to 90.2%.

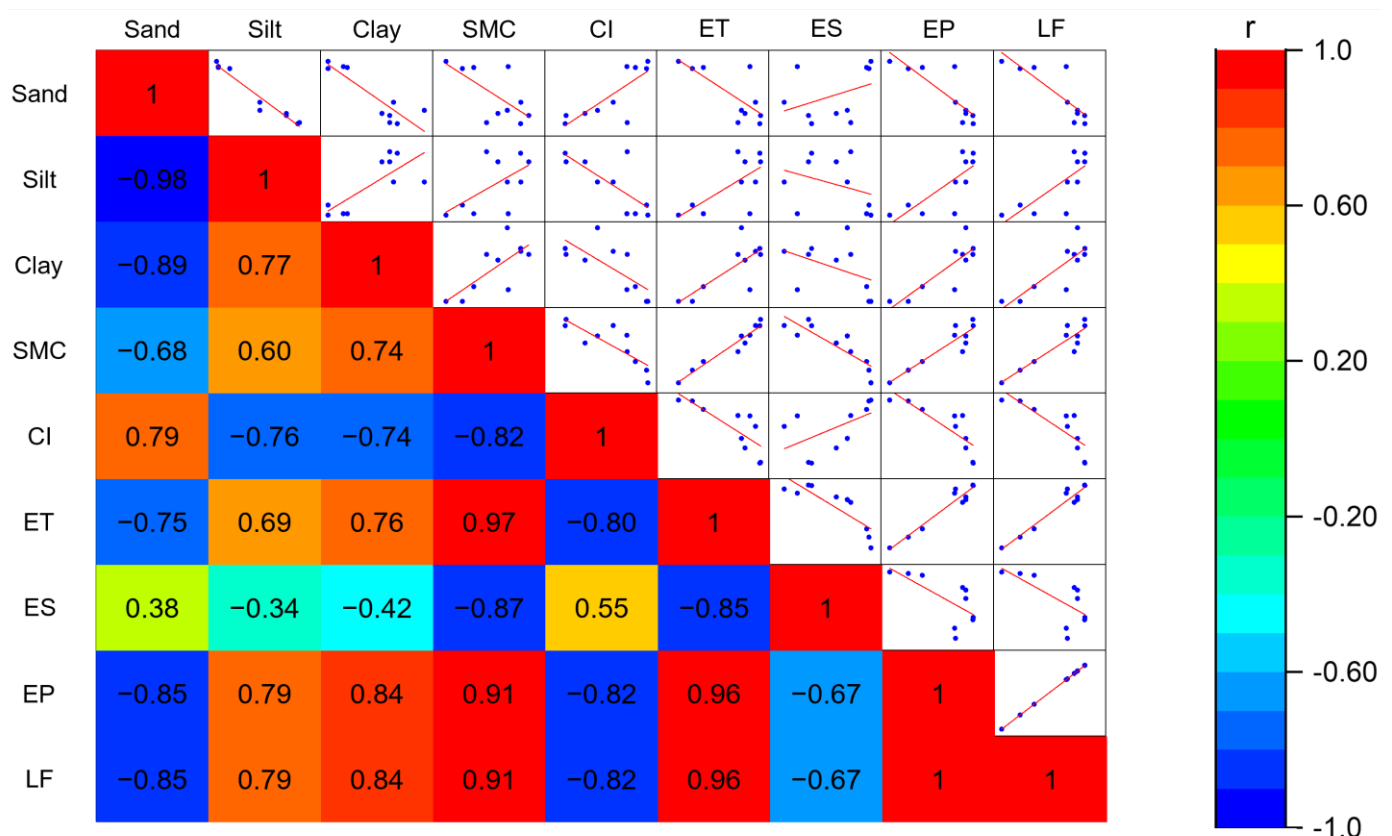
Models A–C represent single-variable regression models for soil physical properties. Model A had the highest R^2 at 0.824, while Model B had the lowest R^2 at 0.678. Model D used SMC and CI as soil variables. The combination of these two soil variables is significant because they can be relatively easily obtained through field sensors. However, Model D's adjusted R^2 of 0.800 was slightly lower than Model A's adjusted R^2 of 0.803, which solely used SMC as a variable. Thus, using both SMC and CI for load estimation may potentially reduce model accuracy. Models E and F utilized soil texture variables. Model E exhibited a higher adjusted R^2 value compared to Model A, while Model F outperformed Model B. Hence, incorporating the sand proportion variable can enhance the accuracy of the regression model. Model G incorporated all soil variables, displaying an adjusted R^2 value of 0.888, which was lower than Model E but higher than Model F. When comparing

Models E and G, the reason for the decrease in model accuracy can be attributed to the fact that the dependent variable is already well explained solely by the SMC variable. A high correlation between the SMC and CI variables can, in fact, decrease model accuracy. Therefore, it is crucial to choose a model with the appropriate number of variables.

Table 6. Regression model for estimating the load factor of the tractor.

Model	Source	Regression Model	R ²	R ² Adj	S.E.
A	f_1	$LF = 0.0147SMC + 0.4487$	0.824	0.803	0.0388
B	f_2	$LF = -0.000255CI + 1.1343$	0.678	0.638	0.0525
C	f_3	$LF = -0.00292S_p + 1.0582$	0.718	0.683	0.0491
D	$f_1 + f_2$	$LF = 0.0114SMC - 0.000076CI + 0.6168$	0.844	0.800	0.0391
E	$f_1 + f_3$	$LF = 0.00997SMC - 0.00147S_p + 0.6719$	0.924	0.902	0.0274
F	$f_2 + f_3$	$LF = -0.000126CI - 0.001804S_p + 1.1130$	0.780	0.717	0.0465
G	$f_1 + f_2 + f_3$	$LF = 0.0108SMC + 0.000030CI - 0.00162S_p + 0.6282$	0.926	0.888	0.0291

Note: SMC = soil moisture content (%), CI = cone index (kPa), S_p = sand proportion (%).



Note: SMC = soil moisture content, CI = cone index, ET = engine torque, ES = engine speed, EP = engine power, LF = load factor. The blue dots in the figure represent each data from 10 sites.

Figure 8. Results of correlation analysis of soil physical properties and engine load characteristics.

Table 7 displays the results of ANOVA analysis for each regression model, showcasing the degrees of freedom (Df), sum of squares (SS), and mean squares (MS). A higher F-value implies that the regression model better explains the variability in the dependent variable. Models E and A exhibited higher F-values of 42.278 and 37.381, respectively, indicating strong explanatory power. In contrast, Models F and B demonstrated lower F-values of 12.375 and 16.848, respectively, indicating relatively weaker explanatory capabilities. Consequently, the SMC is significantly more effective in explaining the load rate compared to the CI. Model G, which utilized all soil variables, yielded an F-value of 24.881. The p -value, calculated using the F-value and Df, indicates the probability that the model's

dependent variable and independent variable have no significant correlation. All models demonstrated statistical significance with $p < 0.01$. Variance inflation factor (VIF) is used for diagnosing multicollinearity, and it is the reciprocal of tolerance. VIF values closer to 1 indicate that there is no correlation between independent variables. Typically, a VIF of 10 or higher suggests multicollinearity [30]. The VIF for each model ranged between 1.854 and 4.435. Therefore, all models did not exhibit multicollinearity issues.

Table 7. ANOVA results for each regression model.

Model		Degrees of Freedom (Df)	Sum of Squares (SS)	Mean Squares (MS)	F-Value	p-Value	Variable	Tolerance	Variance Inflation Factor (VIF)
A	Regression	1	0.0565	0.0565	37.381	0.000 *	SMC		
	Residual	8	0.0120	0.0015					
B	Regression	1	0.0464	0.0464	16.848	0.003 *	CI		
	Residual	8	0.0221	0.0028					
C	Regression	1	0.0492	0.0492	20.370	0.002 *	Sand		
	Residual	8	0.0193	0.0024					
D	Regression	2	0.0578	0.0289	18.964	0.001 *	SMC	0.331	3.201
	Residual	7	0.0107	0.0015			CI	0.331	3.201
E	Regression	2	0.0633	0.0316	42.278	0.000 *	SMC	0.539	1.854
	Residual	7	0.0052	0.0007			Sand	0.539	1.854
F	Regression	2	0.0534	0.0267	12.375	0.005 *	CI	0.370	2.703
	Residual	7	0.0151	0.0022			Sand	0.370	2.703
G	Regression	3	0.0634	0.0211	24.881	0.001 *	SMC	0.329	3.042
							CI	0.225	4.435
	Residual	6	0.0051	0.0008				Sand	0.367

* Significant at $p < 0.01$.

4. Discussion

The data obtained from previous studies were utilized to validate the regression models derived in this study [31]. The study evaluated the tractor's operational performance using the same tractor–moldboard plow combination. In contrast to this study, the moldboard plow had six blades and the tractor had a rated power of 42 kW. The soil physical properties were determined by measuring the SMC in the 150 to 200 mm layer and the CI as the average value in the 0 to 150 mm range, aligning with our data collection methodology for this study. The LF used measurements obtained under the condition of a working depth of 16 cm. The average LF for each soil physical characteristic reported in the previous studies is presented in Table 8.

Table 8. Average LF by soil physical properties for model validation [31].

Site	SMC (%)	CI (kPa)	Soil Texture			LF
			Sand (%)	Silt (%)	Clay (%)	
1	19.45	689.69	68	20	21	0.793
2	24.50	563.21	40	48	12	0.852
3	20.24	864.67	40	28	32	0.921

Table 9 illustrates the estimation value and analysis result of error for the model. The estimated average LF ranged from 0.734 to 0.956 at site 1, 0.808 to 0.991 at site 2, and 0.746 to 0.942 at site 3. MAPE, RMSE, and RD were used as an indicator to evaluate the model performance. The MAPE ranges of models A to G varied from 5.36% to 12.55%. With the exception of one case, Models D to G, which employed multiple soil variables, exhibited lower MAPEs compared to models A to C that utilized single soil variables. This suggests that employing multiple soil variables can enhance the estimative accuracy of the models. However, in the case of Model F, which used CI and sand proportion as variables, its MAPE was higher compared to the model C concerning the sand proportion. This underscores the fact that not all variables hold equal importance, and the choice of specific soil variables can significantly impact the model's performance. Furthermore, this emphasizes the conclusions drawn from the research in the Results section.

Table 9. Analysis of errors in validation data for each regression model.

	Items	Model A	Model B	Model C	Model D	Model E	Model F	Model G
Site 1	Average LF (Kim et al. [31])				0.793			
	Estimated LF	0.734	0.956	0.860	0.787	0.766	0.902	0.748
	Error (%)	7.43	20.58	8.47	0.80	3.44	13.79	5.64
Site 2	Average LF (Kim et al. [31])				0.852			
	Estimated LF	0.808	0.991	0.942	0.855	0.857	0.970	0.844
	Error (%)	5.20	16.21	10.47	0.26	0.57	13.77	1.00
Site 3	Average LF (Kim et al. [31])				0.921			
	Estimated LF	0.746	0.914	0.942	0.783	0.815	0.932	0.807
	Error (%)	19.09	0.84	2.19	15.02	11.58	1.11	12.43
Average	MAPE (%)	10.57	12.55	7.04	5.36	5.19	9.56	6.35
	RMSE	0.110	0.124	0.065	0.080	0.064	0.093	0.071
	RD (%)	12.87	14.44	7.66	9.35	7.44	10.85	8.31

The analysis result of RMSE and RD differed somewhat from MAPE. Model C demonstrated the second lowest values for RMSE and RD. This is the result of RMSE and RD being more responsive to outliers compared to MAPE. In practice, Models D, F, and G, which employed multiple soil variables, exhibited higher errors at specific sites. These results underscore the need for a more diverse dataset of LF data collected under various soil conditions to enhance the model's stability and applicability.

5. Conclusions

In this study, the effect of soil physical properties on LF of tractor engine was analyzed. A correlation analysis was performed between LF and five soil variables: SMC, CI, sand proportion, silt proportion, and clay proportion, and all soil variables were found to have a strong correlation with LF. However, the correlation coefficients between each soil variable and LF were different, indicating that the soil variables had different impacts. The LF estimation model was developed through a regression model using soil variables. The objective of developing this estimation model was to estimate the LF more accurately and compare the accuracy of models using a single soil variable and models using multiple soil variables. In many cases, models using multiple soil variables demonstrated higher accuracy compared to those using a single soil variable. Therefore, adding soil variables allows us to encompass the complexity and variability caused by soil conditions during actual tractor operations, leading to an improvement in model accuracy. However, in some instances, the addition of soil variables led to a decrease in model accuracy. This occurred due to the added soil variable having a relatively low correlation with LF, which increased the error of the model, or the increase in outlier values due to the high correlation between the added variables. Consequently, it was concluded that selecting an appropriate level of model complexity is crucial.

Kim et al.'s (2022) model validation was performed using soil physical properties and LF data reported in [31]. The MAPE of the models varied between 5.19 and 12.55%, with models using multiple soil variables tending to have lower errors. This supports the conclusions of this study. However, there was no correlation between the model's high R^2 value and the error in the verification results. Differences in tractor power, soil consolidation tools, range of soil conditions, etc., can affect the accuracy of the model. Therefore, LF data collected under a wider range of operating conditions and soil conditions are needed to improve the model's reliability and versatility. Research on data collection for these various conditions will continue to be conducted in future studies.

Author Contributions: Conceptualization, W.-S.K. and Y.-J.K.; methodology, W.-S.K.; software, Y.-S.M., Y.-S.K. and R.-G.L.; validation, Y.-S.K.; formal analysis, Y.-S.M. and T.-J.K.; investigation, Y.-S.M. and T.-J.K.; data curation, W.-S.K. and R.-G.L.; writing—original draft preparation, Y.-S.M. and W.-S.K.; writing—review and editing, Y.-S.M. and W.-S.K.; supervision, W.-S.K. and Y.-J.K.; project administration, Y.-J.K. and R.-G.L.; funding acquisition, Y.-J.K. All authors have read and agreed to the published version of the manuscript.

Funding: This work was carried out with the support of "Cooperative Research Program for Agriculture Science and Technology Development (Project No. PJ0156952022)" Rural Development Administration, Republic of Korea.

Institutional Review Board Statement: Not applicable.

Informed Consent Statement: Not applicable.

Data Availability Statement: The data presented in this study are available within the article.

Conflicts of Interest: The authors declare no conflict of interest.

References

1. Zhang, L.; Xu, M.; Chen, H.; Li, Y.; Chen, S. Globalization, green economy and environmental challenges: State of the art review for practical implications. *Front. Environ. Sci.* **2022**, *10*, 870271. [CrossRef]
2. National Institute of Environmental Research Center (NIER). *Standard Operations Procedure for the Construction of Supporting Data for National Air Pollutant Emissions*; NIER: Incheon, Republic of Korea, 2019; Available online: <https://www.air.go.kr/article/view.do?boardId=8&articleId=89&boardId=8&menuId=49¤tPageNo=1> (accessed on 25 September 2023).
3. National Air Emission Inventory and Research Center (NAIR). *Handbook of Estimation Methods for National Air Pollutant Emissions V*; NAIR: Cheongju, Republic of Korea, 2022; Available online: <https://www.air.go.kr/article/view.do?boardId=8&articleId=238&boardId=8&menuId=49¤tPageNo=1> (accessed on 25 September 2023).
4. National Air Emission Inventory and Research Center (NAIR). *2019 National Air Pollutant Emissions*; NAIR: Cheongju, Republic of Korea, 2022; Available online: <https://www.air.go.kr/article/view.do?boardId=7&articleId=145&boardId=7&menuId=48¤tPageNo=1> (accessed on 25 September 2023).
5. National Institute of Agricultural Sciences (NIAS). *2019 Investigation of Agricultural Machinery Usage*; NIAS: Wanju, Republic of Korea, 2020.
6. Kim, W.S.; Lee, S.E.; Baek, S.M.; Baek, S.Y.; Jeon, H.H.; Kim, T.J.; Lim, R.G.; Choi, J.Y.; Kim, Y.J. Evaluation of exhaust emissions factor of agricultural tractors using portable emission measurement system (PEMS). *J. Drive Control* **2023**, *20*, 15–24.
7. Zhang, G.; Sandanayake, M.; Setunge, S.; Li, C.; Fang, J. Selection of emission factor standards for estimating emissions from diesel construction equipment in building construction in the Australian context. *J. Environ. Manag.* **2017**, *187*, 527–536. [CrossRef] [PubMed]
8. Lee, J.H.; Jeon, H.H.; Baek, S.Y.; Baek, S.M.; Kim, W.S.; Siddique, M.A.A.; Kim, Y.J. Analysis of Emissions of Agricultural Tractor according to Engine Load Factor during Tillage Operation. *J. Drive Control* **2022**, *19*, 54–61.
9. Tan, D.; Tan, J.; Peng, D.; Fu, M.; Zhang, H.; Yin, H.; Ding, Y. Study on real-world power-based emission factors from typical construction machinery. *Sci. Total Environ.* **2021**, *799*, 149436. [CrossRef] [PubMed]
10. Lee, S.E.; Kim, T.J.; Kim, Y.J.; Lim, R.G.; Kim, W.S. Analysis of Engine Load Factor for Agricultural Cultivator during Plow and Rotary Tillage Operation. *J. Drive Control* **2023**, *20*, 31–39.
11. Baek, S.M.; Kim, W.S.; Baek, S.Y.; Jeon, H.H.; Lee, D.H.; Kim, H.K.; Kim, Y.J. Analysis of engine load factor for a 78 kW class agricultural tractor according to agricultural operations. *J. Drive Control* **2022**, *19*, 16–25.
12. Lee, D.I.; Park, J.; Shin, M.; Lee, J.; Park, S. Characteristics of Real-World Gaseous Emissions from Construction Machinery. *Energies* **2022**, *15*, 9543. [CrossRef]
13. Shin, D.H.; Park, Y.S.; Yoo, C.; Park, S.H. Study on Real-Work NOx Emission Characteristics according to Load Factor of Excavator. *J. Drive Control* **2023**, *20*, 1–8.
14. Barati, K.; Shen, X. Operational level emissions modelling of on-road construction equipment through field data analysis. *Autom. Constr.* **2016**, *72*, 338–346. [CrossRef]
15. Koo, Y.M. PTO torque and draft analyses of an integrated tractor-mounted implement for round ridge preparation. *J. Biosyst. Eng.* **2022**, *47*, 330–343. [CrossRef]
16. Kim, J.T.; Im, D.; Cho, S.J.; Park, Y.J. A Study on the Prediction of Driving Performance of Agricultural Tractors Driving on Dry Sand. *J. Biosyst. Eng.* **2022**, *47*, 502–509. [CrossRef]
17. Inchebron, K.; Seyedi, S.M.; Tabatabaekoloor, R. Performance evaluation of a light tractor during plowing at different levels of depth and soil moisture content. *Int. Res. J. Appl. Basic Sci.* **2012**, *3*, 626–631.
18. Kim, W.S.; Kim, Y.J.; Park, S.U.; Kim, Y.S. Influence of soil moisture content on the traction performance of a 78-kW agricultural tractor during plow tillage. *Soil Tillage Res.* **2021**, *207*, 104851. [CrossRef]

19. Rasool, S.; Raheman, H. Improving the tractive performance of walking tractors using rubber tracks. *Biosyst. Eng.* **2018**, *167*, 51–62. [[CrossRef](#)]
20. Battiato, A.; Diserens, E. Tractor traction performance simulation on differently textured soils and validation: A basic study to make traction and energy requirements accessible to the practice. *Soil Tillage Res.* **2017**, *166*, 18–32. [[CrossRef](#)]
21. Han, G.; Kim, K.D.; Ahn, D.V.; Park, Y.J. Comparative Analysis of Tractor Ride Vibration According to Suspension System Configuration. *J. Biosyst. Eng.* **2023**, *48*, 69–78. [[CrossRef](#)]
22. Choudhary, S.; Upadhyay, G.; Patel, B.; Naresh; Jain, M. Energy requirements and tillage performance under different active tillage treatments in sandy loam soil. *J. Biosyst. Eng.* **2021**, *46*, 353–364. [[CrossRef](#)]
23. Ayers, P.D.; Perumpral, J.V. Moisture and density effect on cone index. *Trans. ASAE* **1982**, *25*, 1169–1172. [[CrossRef](#)]
24. *ASABE Standards EP542*; Procedure for Using and Reporting Data Obtained with the Soil Cone Penetrometer. American Society of Agricultural and Biological Engineers: St. Joseph, MO, USA, 2019.
25. Reicosky, D. *Managing Soil Health for Sustainable Agriculture Volume 2: Monitoring and Management*; Burleigh Dodds Science Publishing: Cambridge, UK, 2018.
26. Tan, K.H. *Soil Sampling, Preparation, and Analysis*; CRC Press: New York, NY, USA, 1995; ISBN 0-8247-9675-6.
27. Kim, W.S.; Lee, D.H.; Kim, Y.J.; Kim, Y.S.; Park, S.U. Estimation of Axle Torque for an Agricultural Tractor Using an Artificial Neural Network. *Sensors* **2021**, *21*, 1989. [[CrossRef](#)]
28. Kim, W.S.; Kim, Y.J.; Baek, S.Y.; Baek, S.M.; Kim, Y.S.; Choi, Y.; Kim, Y.K.; Choi, I.S. Traction performance evaluation of a 78-kW-class agricultural tractor using cone index map in a Korean paddy field. *J. Terramechanics* **2020**, *91*, 285–296. [[CrossRef](#)]
29. Chancellor, W.; Thai, N. Automatic control of tractor transmission ratio and engine speed. *Trans. ASAE* **1984**, *27*, 642–646. [[CrossRef](#)]
30. Salmerón Gómez, R.; Rodríguez Sánchez, A.; García, C.G.; García Pérez, J. The VIF and MSE in Raise Regression. *Mathematics* **2020**, *8*, 605. [[CrossRef](#)]
31. Kim, Y.S.; Lee, S.D.; Baek, S.M.; Baek, S.Y.; Jeon, H.H.; Lee, J.H.; Kim, W.-S.; Shim, J.Y.; Kim, Y.J. Analysis of the effect of tillage depth on the working performance of tractor-moldboard plow system under various field environments. *Sensors* **2022**, *22*, 2750. [[CrossRef](#)]

Disclaimer/Publisher’s Note: The statements, opinions and data contained in all publications are solely those of the individual author(s) and contributor(s) and not of MDPI and/or the editor(s). MDPI and/or the editor(s) disclaim responsibility for any injury to people or property resulting from any ideas, methods, instructions or products referred to in the content.